THE INTERNATIONAL JOURNAL OF SCIENCE & TECHNOLEDGE

Theoretical Study of the Parameters Affecting Vane Tip Friction in Oil Vane Pumps Using Simplified Tehl-Model

Mohamed Wasel
Professor, Faculty of Engineering, Department of Mechanical Power Engineering, Mansoura University, Mansoura, Egypt
Abdel-Rahim A. Abdel-Rahim
Professor, Faculty of Engineering, Department of Mechanical Power Engineering, Mansoura University, Mansoura, Egypt
Hany El-Gohary
Assistant Professor, Faculty of Petroleum and Mining Engineering, Department of Engineering Science, Suez University, Suez, Egypt
Mohamed Elashmawy
Assistant Professor, Faculty of Petroleum and Mining Engineering, Department of Engineering Science, Suez University, Suez, Egypt

Abstract:
A simple (Thermo-Elasto-Hydrodynamic Lubrication) TEHL-Model was developed to calculate the friction forces between vane tip and cam-ring in oil vane pumps. The incentive of this work is to present an effective and sim-ple tool that helps vane pump designers to make a primary study of the effect of important parameters on the friction coefficient between vane tip and cam-ring. Such parameters are relative vane tip speed, normal vane force and vane tip radius of curvature. Navier-Stokes and energy equations were numerically solved using a finite difference tech-nique. The viscosity and density distributions as a function of pressure and temperature were taken into consideration. The results show that the effect of the normal vane force is very small compared to the relative speed. The vane tip relative speed should be higher than 4.8 m/s for reduced vane tip friction. Increasing of van tip radius of curvature and relative speed as well as decreasing of normal vane force, increases the lubricant oil film thickness and decreases the vane tip friction coefficient. It is feasible to concentrate future studies to include the effect of the material surface properties into TEHL-Model.

Keywords: *Vane pump, friction, friction coefficient, TEHL, hydraulic, vane tip, film thickness*

1. Introduction

The friction force between vane tip and cam-ring is relatively high compared with other friction sources in the vane pump. Trying to understand the nature and behavior of such friction is very important to minimize it. Decreasing vane tip friction enhances vane pump performance which leads to less fuel consumption in the automobiles.
Many parameters affecting the vane pump performance was theoretically and experimentally studied by others. The following parameters were selected:

1.1. Vane Tip Geometry

A computer model was developed using a mixed lubrication model to investigate the tribological performance of blade and liner interface in a transfer pump lubricated with diesel fuel (Sui 1995). Results show that increasing the blade surface radius also greatly improves the film parameter and reduces the interfacial friction by as much as 80 percent.
The suitable contact force of the vane tip against cam-ring together with properly determined system geometry, have a significant influence on achieving high efficiency and life of the pump (Panek 2004). In order to achieve this purpose, it is necessary to determine the master value of the contact force that the system must generate.
By increasing vane thickness, vane pump efficiency did not. It is known that increasing vane thickness will lead to an increase of vane normal force which may increase vane friction. The important parameter should be considered for the efficiency of the balanced vane pump is denoted by ε and defined as the ratio of vane pump lift to vane thickness. Reducing friction coefficient and increasing ε is the key parameters to increase the pump efficiency (Inaguma 2010). In 2014 an experimental and theoretical study for the effect of the

ratio of vane pump lift to vane thickness (ε) on vane tip friction torque was tested. Results show that the variation of the vane friction torque is increased by increasing of ε (Inaguma and Yoshida 2014).
Increasing of vane tip radius of curvature enhances lubrication conditions between vane tip and cam-ring in oil vane machines. However increasing of vane thickness increases vane friction at low oil temperatures and enhances oil lubrication conditions at higher temperatures. Authors recommend keeping vane radius of curvature and vane thickness higher than 2mm and 1.5mm respectively (Elashmawy and Alghamdi 2015).

1.2. Surface Roughness of the Cam-Ring
Results indicated that the film thickness at the blade/liner interface in a transfer pump lubricated with diesel fuel is generally lower than the surface roughness level. Reducing the surface roughness has a significant effect on improving film thickness-to-surface roughness ratio (Sui 1995).
Friction torque arising from the friction between cam contour and vane tip is significant (Inaguma and Hibi 2007). The friction torque was reduced by lessening the surface roughness of the cam contour, resulting in an improvement of mechanical efficiency.

1.3. Coatings
Ion-plated hard and wear-resistant TiN coatings were applied in vane pumps and tested (Gabriel et al. 1983). A wear reduction by a factor of 400 for the coated parts was observed and the uncoated counterparts also showed a decrease in wear by a factor of 60.
(Physical Vapor Deposition), PVD-coated pistons of an axial piston machine using Zircon carbide with graded hardness profile ZrCg as a coating material (Sharf and Murrenhoff 2006) reveal limited wear within the first hours of operation and very low friction between piston and bushing.
A comparison was performed between five different PVD-coated vane tips and the normal vane without coating (Elashmawy and Murrenhoff 2009). The results show that the effect of the normal vane force and the pressure difference between the two sides of the vane are very small compared to the vane tip relative speed. Coating material shows no significant effect on the friction coefficient in oil vane pumps.

1.4. Oil Temperature
In case of vane pump low temperature regions; increasing oil temperature will decrease friction and enhance efficiency. While in high temperature regions increasing of oil temperature will not decrease friction and the efficiency will not increase (Inaguma 2011). A study concerning oil temperature effect on both internal gear and vane pumps was performed in Japan. Results showed that the overall efficiency of both the internal gear and balanced vane pumps decreases at very low and very high oil temperatures. 80°C is recommended for higher overall pump efficiency. (Inaguma and Yoshida 2013).
In the present study the friction force between vane tip and cam-ring is theoretically calculated. A simple TEHL-Model developed by authors is used. The validation of this model was tested using the experimental results previously obtained by Elashmawy and Murrenhoff (2009). The effect of some parameters on the friction coefficient was studied. These parameters are the relative speed between vane tip and cam-ring, normal vane force, and vane tip radius of curvature. The essential distinction between this study and the previous studies is the simplicity of the model with relatively acceptable deviation from experimental results.

2 Simulation and Modelling of Smooth Contact Between Vane Tip and Cam-Ring

2.1 Pressure Distribution and Film Thickness
Figure 2 shows a comparison between Hertzian pressure distribution and the exact solution of the TEHL-Model by solving Reynolds Equation with elastic deformation. The area of interest will be assumed as parallel, just to simplify the model. Under this approximation the Reynolds equation Eq. 1 and the deformation equation Eq. 2 will not be solved in the present study.

$$\frac{dP}{dx} = 12\,\mu\, u\left(\frac{h(x)-h_o}{h(x)^3}\right) \qquad (1)$$

$$h(x) = h_{min} + \frac{x^2}{2R} - \frac{2\left(1-\upsilon^2\right)}{\pi E}\int_{-\infty}^{\infty} P(s)\,ln\left(x-s\right)^2\,ds \qquad (2)$$

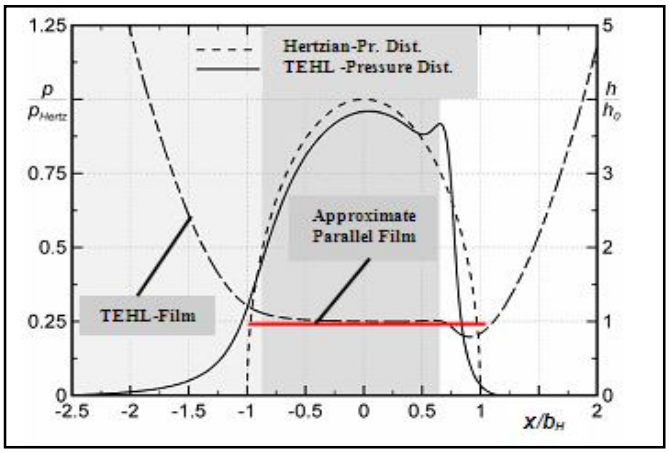

Figure 1: Comparison between typical and approximated pressure and film thickness distribution in the TEHL contact (Faber 2006)

In this model the area of flow will be considered as a parallel area using Hertz theory to predict the pressure distribution "elliptic curve", Eq. 7, Fig. 2 and using Hamrock /Dowson formula (Gold 2003) to predict the lubricant mean film thickness, Eq. 8.

$$P_H = \sqrt{\frac{F\,E^{'}}{2\pi R\, l_{eff}}} \tag{3}$$

$$b_H = \sqrt{\frac{8F\,R}{\pi E^{'} l_{eff}}} \tag{4}$$

$$E = \frac{2E_1 E_2}{E_1 + E_2} \tag{5}$$

$$E^{'} = \frac{E}{(1-\upsilon^2)}, \quad \upsilon = 0.3 \tag{6}$$

$$P(x) = P_H \sqrt{1-\left(\frac{x}{b_H}\right)^2} \tag{7}$$

$$h_o = 2.69 G^{0.53} U^{0.67} W^{-0.067} R \tag{8}$$

Where G: Material parameter, U: Speed parameter, W: Load parameter, and R: Reduces radius of curvature.

$$G = \alpha_p E^{'} \tag{9}$$

$$U = \frac{\mu_o u}{2E^{'}R} \tag{10}$$

$$W = \frac{F}{E^{'} R\, l_{eff}} = 2\pi\left(\frac{P_H}{E^{'}}\right)^2 \tag{11}$$

$$R = \frac{R_1 R_2}{R_1 + R_2} \tag{12}$$

2.2. Velocity Distribution within Lubricant Film

Navier-Stokes equation, Eq. 13 is used to calculate the velocity distribution within the lubricant film of the smooth contact between vane tip and cam-ring.

$$\frac{\partial P}{\partial x} = \mu\left(\frac{\partial^2 u}{\partial y^2}\right) + \frac{\partial \mu}{\partial y}\left(\frac{\partial u}{\partial y}\right) \tag{13}$$

2.2.1. Assumptions

- Steady flow
- Two-dimensional flow in x and y directions
- Velocity in y direction is considerably smaller than in the x direction, $v << u$.
- The gradients of the first and higher order of velocity in x direction is considerably smaller than in the y direction.

- The pressure change in y direction is extremely insignificant.

2.3. Temperature Distribution within lubricant Film

Energy equation in its simple two dimensional form, Eq. 14 is used to calculate the temperature distribution in the lubricant oil film. The specific heat of oil was taken as $c_p = 2000\ J/kgK$.

$$-\rho c_p\left(u\frac{\partial T}{\partial x}+v\frac{\partial T}{\partial y}\right)-\frac{uT}{\rho}\frac{\partial \rho}{\partial T}\frac{\partial P}{\partial x} + k\left(\frac{\partial^2 T}{\partial y^2}\right)+\mu\left(\frac{\partial u}{\partial y}\right)^2=0 \quad (14)$$

2.3.1. Boundary Conditions

$$T = T_o \quad for\ x \to -\infty \quad (15)$$

The upper and lower boundaries are the surface temperatures of vane tip and cam-ring. For the present work the wall temperatures were assumed to be constant and equal to the oil temperature, T_o.

Conduction heat transfer coefficient for oil was taken according to Rodermund, Eq. 16 (Ortwig 1992).

$$k = k_o\left(1+10^{-4}\frac{P-P_o}{P_o}\right) \quad (16)$$

with: $k_o = 0.15\ W/mK$

2.4. Oil Rheology

The oil type used was HLP46, mineral oil. The dynamic viscosity and density of this oil at T=40°C are μ=0.04 Pa.s and ρ=865 kg/m3 respectively.

2.4.1. Viscosity

Viscosity dramatically increases by increasing the pressure and decreases by increasing the temperature. So that the relation ship govern this dependence is very important for theoretical calculations. According to Blume correlation (1987), the physical constants used in this correlation are classified according to pressure level as low pressure region (up to 1000 bar) and high pressure region (over 1000 bar). Table 1 defines the constants of Eq. 17 at low and high regions.

$$ln\,\mu_{T,P} = ln\,K_{p_o} + \frac{B_{p_o}}{T+C} + P\left[\alpha_{T_o}+\frac{\Delta B}{\Delta P}\left(\frac{1}{T+C}-\frac{1}{T_o+C}\right)\right] \quad (17)$$

With $C = 95\ ^oC,\ P_o = P_{atm}, and\ T_o = 0\ ^oC$

FVA2	K_{P_o} [cp]	B_{P_o} [°C]	α_{T_o} [10^{-3}/bar]	$\Delta B/\Delta P$ [°C/bar]	Error [%]
$p \le 10^3$	*0.144*	*754.5*	*3.0051*	*0.33613*	*1.15*
$p > 10^3$	*0.240*	*720.8*	*2.8206*	*0.32838*	*4.55*

Table 1: Constants of Eq. 17 at low and high pressures

2.4.2. Density

Oil density was calculated according to Blume (1987). It is also divided into two pressure regions.

$$\rho_{T,P} = \rho_{o,o} + T\alpha_{T_o,0bar} + P\alpha_{P,0^oC} + PT\frac{\Delta\alpha_p}{\Delta T} \quad (18)$$

FVA2	$\rho_{o,o}$	$\alpha_{T_o,0bar}$ [10^{-4}]	$\alpha_{P,0^oC}$ [10^{-5}]	$\Delta\alpha_p/\Delta T$ [10^{-7}]	Error [%]
$p \le 10^3$	*0.88*	*-5.54*	*4.2565*	*1.101*	*0.25*
$p > 10^3$	*0.90*	*-5.77*	*2.3967*	*0.984*	*1.1*

Table 2: Constants of Eq. 18 at low and high pressures

2.5. Vane Tip Friction Force

The friction between vane tip and cam-ring was assumed as smooth contact friction due to oil shear only. The equations used are as follows:

$$\tau = \mu \frac{\partial u}{\partial y}\bigg|_{wall} \tag{19a}$$

$$\frac{dF_{fr}}{l_{eff}} = \tau dx + P dh \Leftrightarrow \frac{F_{fr}}{l_{eff}} = \int_{-\infty}^{\infty} \tau dx + \int_{-\infty}^{\infty} P \frac{dh}{dx} dx \tag{19b}$$

$$\lambda = \frac{|F_{fr}|}{F} \tag{20}$$

2.6. Numerical Concept

Numerical solution using finite difference technique was used. The lubricant film assumed to be parallel, so that the physical domain is rectangular, and there is no need to perform any transformations to computational domain, this will simplify the model. The pressure distribution along the x-axis was taken according to Hertz equation, Eq. 7. The mesh independent solution shows that, *60X10* points are sufficient. Table 3 shows the mesh independent results behavior.

Grid Points	λ	T_{max} **@x/b$_H$=0**
200	0.080	78.41
300	0.081	78.46
400	0.081	78.48
500	0.082	78.48
600	0.082	78.49
700	0.082	78.49
800	0.082	78.49

Table 3: Mesh size independent of numerical solution

3. TEHL-Model Validation

TEHL-Model validation was performed by comparing the computed results with the available experimental results, Fig. 3. The comparison was performed at a constant speed of 2000 rpm (4.8 m/s) and show the effect of normal vane force on vane tip friction coefficient. At low normal vane forces, TEHL model results show that the friction coefficient goes to ∞ with the normal vane force approaches to zero.

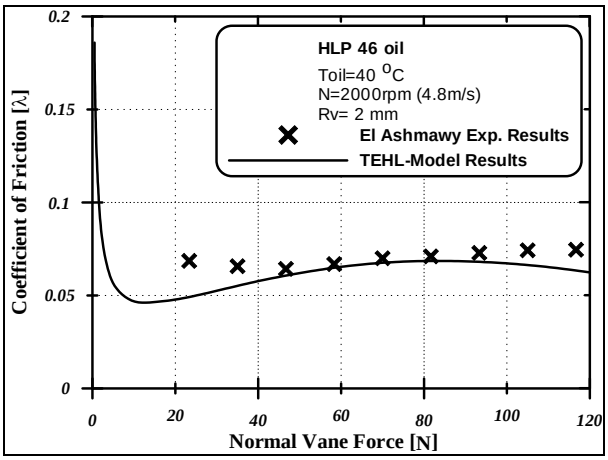

Figure 2: TEHL-model validation, coefficient of friction vs. normal vane force

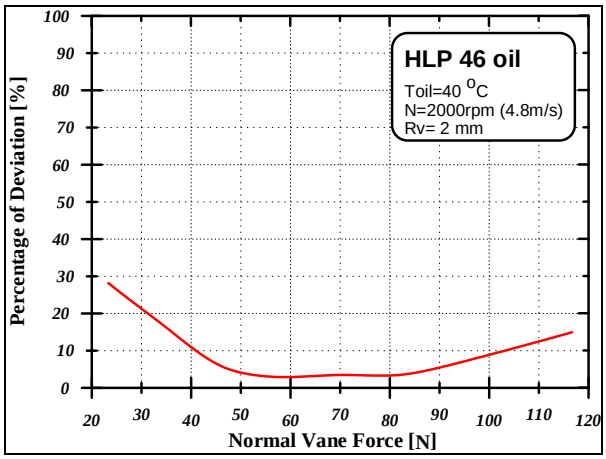

Figure 3: Deviation behavior between TEHL model and experimental results at constant speed of 2000 rpm

Figure 4 shows the deviation behavior between TEHL-Model and experimental results obtained by Elashmawy (2009), Fig. 3. The deviation analysis show relatively good matching especially at the margin from 40 up to 100N.

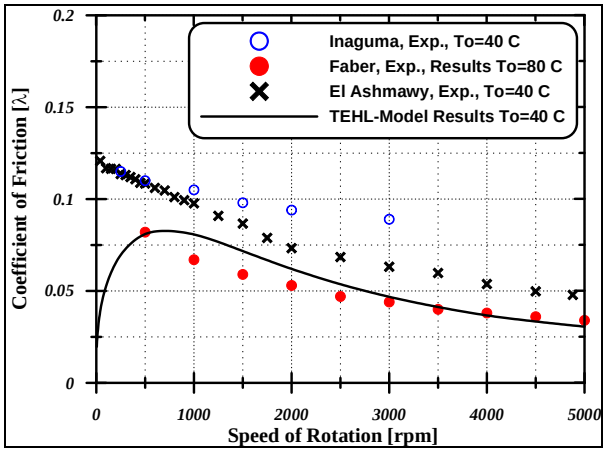

Figure 4: TEHL-model validation, coefficient of friction vs. speed of rotation

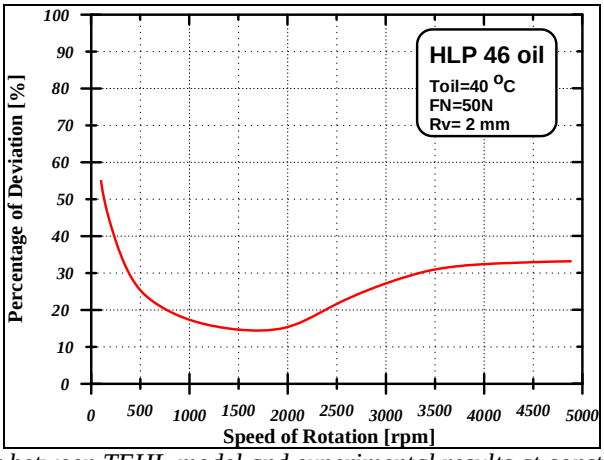

Figure 5: Deviation behavior between TEHL-model and experimental results at constant vane normal force of 50N

Figure 5 shows a comparison between TEHL-Model and Elashmawy (2009), Faber (2006) and Inaguma (2005) results. The comparison show that at high speed region ≥ 2.4 m/s, ($N \geq 1000$ rpm), the behavior of TEHL-Model results are relatively good matched with experimental results. While at the low speed region ($N < 1000$ rpm) results show bad matching with experimental results. So that the low speed region results should not be considered.

The friction coefficient of the high speed region lies within the margin of mixed friction, $\lambda = 0.01 - 0.1$, (Gold 2003). For mixed friction, part of friction is due to fluid friction and the other part is due to material friction which is not considered by TEHL-Model, this explains why all curves at high speed region lay under the experimental results.

Within the low speed region, especially with increasing of normal vane force, the friction coefficient moves toward the boundary friction region, $\lambda = 0.1 - 0.2$, (Gold 2003). For boundary friction the share of friction due to material friction is much more compared with mixed friction. Figure 6 shows the deviation behavior between TEHL-Model and experimental results obtained by Elashmawy (2009), Fig. 5. The deviation of results at low speed region increases rapidly with decreasing of rotational speed. At the margin of very low speeds the deviation goes to infinity. Based on deviation analysis, all results that lie within the low speed region (boundary friction) should not be considered.

4. Results and Discussion

4.1. Effect of Relative Speed on Friction Coefficient

Figure 7 shows the effect of relative speed on the friction coefficient. The curves at the high speed region show that increasing speed of rotation decreases the vane tip friction coefficient. Most curves intersect around speed of 2000 rpm which gives an indication that the speed of rotation should not be less than 2000 rpm (4.8 m/s) to guarantee good lubrication within vane tip. This indication is the same recommendation obtained by Elashmawy (2009).

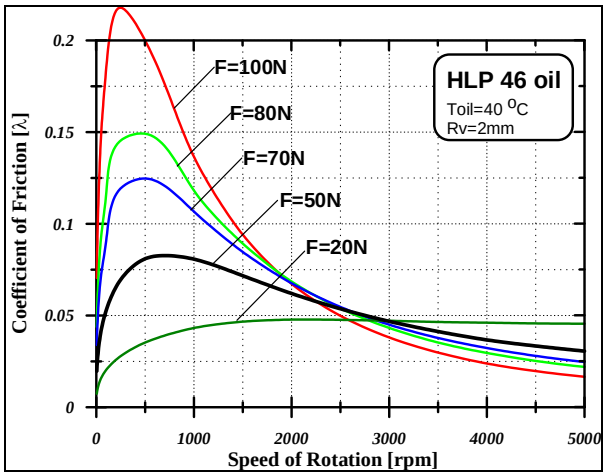

Figure 6: Effect of rotational speed on the coefficient of friction

4.2. Effect of Normal Vane Force on Vane Tip Friction Coefficient

Figure 8 shows the effect of normal vane force on vane tip coefficient of friction. The high speed region shows relatively small effect of normal vane force on the vane tip, friction coefficient compared with low speed region. The curve of Fig. 8 shows unclear trend.

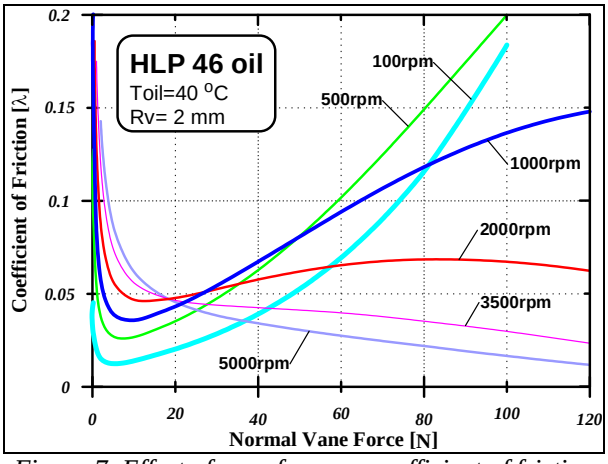

Figure 7: Effect of vane force on coefficient of friction

4.3. Effect of Normal Vane Force and Relative Vane Tip Speed on Average Film Thickness

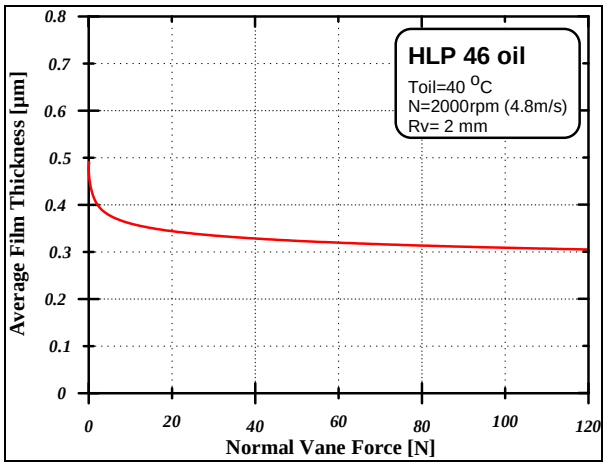

Figure 8: Average film thickness vs. normal vane force

Figure 9 shows that increasing normal vane force decreases average film thickness. The rate of change of film thickness in the region from 0 up to 10 N normal vane force is very high. While it is relatively small after 10 N. High values of normal vane force is not recommended, but it is important to satisfy vane tip tightness to enhance pump volumetric efficiency.

Unlike normal vane force effect, increasing relative vane tip speed increases the average film thickness, Fig. 10. High speed of rotations is recommended for oil vane pump applications.

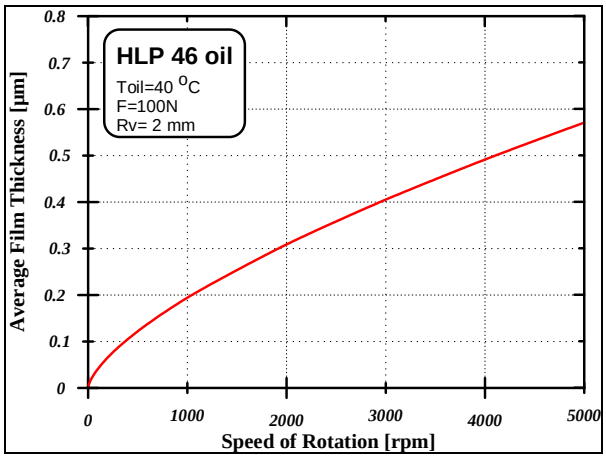

Figure 9: Average film thickness vs. speed of rotation

4.4 Effect of Vane Tip Radius on Friction Coefficient and Oil Film Thickness

Vane tip radius of curvature is constrained by the vane geometry. The vane thickness is normally small, depending on vane pump design and delivery pressure. Figure 11 shows the effect of vane tip radius on the coefficient of friction. Increasing vane tip radius of curvature decreases the vane tip coefficient of friction and increases the oil film thickness, Fig. 12.

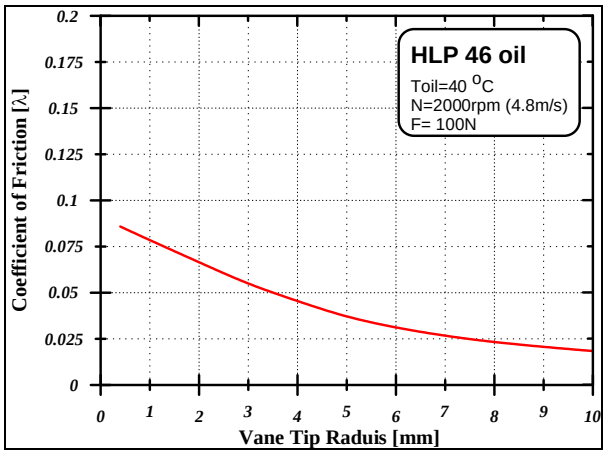

Figure 10: Effect of vane tip radius on vane tip coefficient of friction

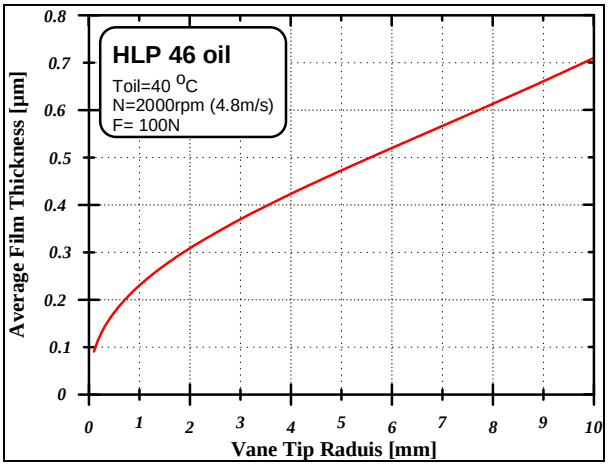

Figure 11: Effect of vane tip radius on average film thickness

4.5. Pressure, Viscosity and Density Distributions

Figure 13 shows Dynamic viscosity and density of the middle film layer versus dimensionless distance. The peak of dynamic viscosity is almost at the center. The dependency of density of pressure and temperature is not so high. The variation is around 100 kg/m^3 along the deformation distance. The peak of density is found also at the centre.

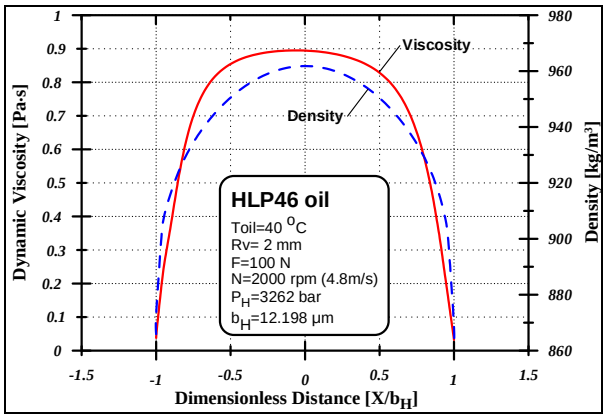

Figure 12: Viscosity and density distribution

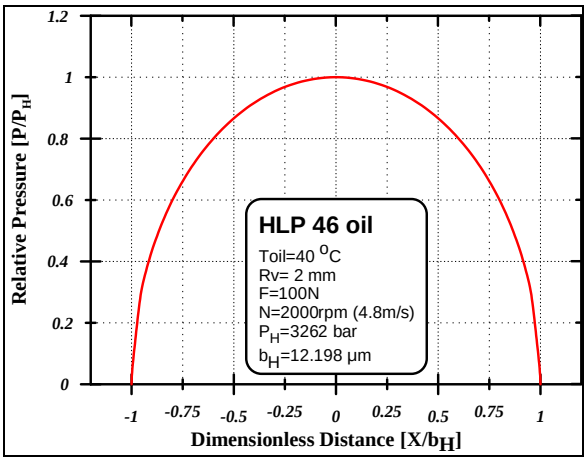

Figure 13: Hertzian pressure distribution

Figure 14 shows the pressure distribution used for TEHL-Model analysis, Hertzian pressure distribution.

5. Conclusions and Recommendations

In the present study a simplified TEHL-Model was developed to investigate the parameters affecting the friction between vane tip and cam-ring within oil vane pumps. HLP46 mineral oil at 40°C was used.

The following conclusions were obtained:

1. Relative speed between vane tip and cam-ring should be higher than 4.8 m/s (2000 rpm) for reduced friction.
2. Increasing of vane tip relative speed and/or decreasing of normal vane force increases vane tip oil film thickness.
3. Increasing of vane tip radius of curvature increases vane tip oil film thickness.
4. TEHL-Model is not sufficient to predict vane tip friction coefficient in the boundary friction regions.
5. The following points are recommended for future work:
6. Increasing of vane tip radius of curvature is recommended. The limitation of radius of curvature due to vane geometry should be carefully studied.
7. More effort trying to consider material friction simultaneously with TEHL-Model is highly recommended for higher loads applications.
8. Because the suction part shows the maximum vane friction, it is feasible to concentrate future studies on reducing vane friction within the suction part.

b_H	Hertzian deformation length	[µm]
c	Specific heat	[J/kgK]
E	Modulus of elasticity	[Pa]
E'	Effective modulus of elasticity	[Pa]
F	Normal vane force	[N]
F_{fr}	Friction vane force	[N]
G	Material parameter	
h_o	Mean film thickness	[µm]
k	Thermal conductivity	[W/mK]
k_o	Thermal conductivity at atmosphere	[W/mK]
l_{eff}	Effective contact length, vane width	[m]
N	Pump speed of rotation	[rpm]
P	System pressure	[bar]
P_H	Hertzian pressure	[bar]
q	Heat flux	[W/m^2]
R	Reduced radius of curvature	
R_V	Vane tip radius of curvature	[mm]
T	Oil temperature	[°C]
T_o	Oil initial temperature	[°C]
T_W	Oil wall temperature	[°C]
T_{max}	Oil maximum temperature, y-axis	[°C]
U	Speed parameter	
u	Oil velocity component, x-axis	[m/s]
v	Oil velocity component, y-axis	[m/s]

W	Load parameter	
Greek Symbols		
λ	Friction coefficient	
μ	Dynamic viscosity	[Pa.s]
υ	Poisson's ratio, 0.3 for steel	
ρ	Density	[kg/m^3]
τ	Shear stress	[N/m^2]

Table 4: Nomenclature

6. References

1. Blume, J. 1987 Druck und Temberatureinfluß auf Viscosität und Kompressibilität von flüssigen Schmierstoffen. RWTH Aachen University Dissertation, Germany.
2. Elashmawy, M. and Alghamdi, A. 2015 Vane Geometry Effect on Lubrication Conditions between Vane Tip and Cam-Ring in Hydraulic Vane Machines. International Journal of Mechanical Engineering and Applications. Special Issue: Advanced Fluid Power Sciences and Technology. Vol. 3, No. 5, pp. 1-10. doi: 10.11648/j.ijmea.s.20150305.11.
3. Elashmawy, M. and Murrenhoff, H. 2009 Experimental Investigation of friction force between vane tip and cam-ring in oil vane pumps, International Journal of Fluid Power, Vol. 10, No. 1, pp 37-46.
4. Faber, Ingo 2006 Theoretische und experimentelle Untersuchung der Flügelkopfreibung in einer Flügelzellenpumpe. Bochum, University Dissertation, Germany.
5. Gabriel, H. M. et al. 1983 Improved component performance of vane pumps by ion-plated TiN coatings. Elsevier, Thin Solid Films, 108 189-197.
6. Gold, P. W. 2003 Tribology. Umdruck zur Vorlesung, Trans-Aix-Press, Aachen, Germany.
7. Inaguma, Y. 2010 Theoritical Analysis of Mechanical Efficiency in Vane Pump. JTEKT Engineering Journal English Edition, No. 1007E,; pp. 28-35.
8. Inaguma, Y. 2011 Oil temperature influence on friction torque characteristics in hydraulic. Proc IMechE Part C: J Mechanical Engineering Science 226(9); pp. 2267-2280.
9. Inaguma, Y. and Hibi, A. 2005 Vane pump theory for mechanical efficiency. Proceedings of the Institution of Mechanical Engineers Part C-Journal of Mechanical Engineering Science, 219 (11), 1269-1278.
10. Inaguma, Y. and Hibi, A. 2007 Reduction of friction torque in vane pump by smoothing cam ring surface. Proceedings of the Institution of Mechanical Engineers Part C-Journal of Mechanical Engineering Science, 221 (5), pp. 527-534.
11. Inaguma, Y. and Yoshida, N. 2013 Mathematical Analysis of Influence of Oil Temperature on Efficiencies in Hydraulic Pumps for Automatic Transmissions. SAE Int. J. Passeng. Cars - Mech. Syst. 6(2):786-797, doi:10.4271/2013-01-0820.
12. Inaguma, Y. and Yoshida, N. 2014 Variation in Driving Torque and Vane Friction Torque in a Balanced Vane Pump. SAE Technical Paper, 2014-01-1764.
13. Ortwig, H. 1992. Theoretical analysis of physical load parameters in the tribological system, vane/cam-ring/hydraulic oil of a vane pump shown. Pt. I: Load calculations of the vane pump shown. Tribologie und Schmierungstechnik, Hannover, 39 (1992) 4, pp. 219-226.
14. Ortwig, H. 1992 Theoretical analysis of physical load parameters in the tribological system vane/cam-ring/hydraulic oil of a vane pump shown. Pt. II: Calculation of the lubricated contact parameters. Tribologie und Schmierungstechnik, Hannover, 39 (1992) 3, pp. 144-151.
15. Ortwig, H. 1992 Pressure and temperature measurements in tribosystem blade/lifting/ring/hydraulic oil of a vane cell pump. Tribologie und Schmierungstechnik, Hannover, 39 (1992) 6, pp. 339-347.
16. Scharf, S. and Murrenhoff, H. 2006 Wear and friction of ZrCg-coated pistons of axial piston pumps. International Journal of Fluid Power, Vol. 7, No. 3, pp. 13-20.
17. Sui, P. C. 1995 Prediction of film thickness and friction at a rotary pump blade and liner interface. American Society of mechanical Engineering (ASME), Vol. 72, ASME, New York, pp. 115-122.